JOURNAL OF CATALYSIS 125, 325–334 (1990)

Adsorption of H_2O and H_2S on Thin Films of Cobalt Oxide Supported on Alumina

E. AUSCHITZKY,* A. B. BOFFA,* J. M. WHITE,* AND T. SAHIN†

*Department of Chemistry, University of Texas, Austin, Texas 78712; and †Department of Chemical Engineering, Montana State University, Bozeman, Montana 59717

Received July 24, 1989; revised May 8, 1990

The interaction of hydrogen sulfide and water with a CoO/Al_2O_3 surface has been examined by Auger electron spectroscopy and temperature-programmed desorption. AES and TPD show that H_2S decomposition occurs readily on CoO/Al_2O_3 at low temperature. For low H_2S exposures at 140 K, no molecular water desorbs in TPD. With large exposures, hydrogen sulfide appears to react with the surface to form water, which is the only product observed. No significant amounts of hydrogen are desorbed. These results are compared with TPD of directly dosed water. © 1990 Academic Press, Inc.

1. INTRODUCTION

Considerable effort has been directed toward improving the efficiency of industrial alumina-based catalysts (*1–7*). The commercial hydrotreating catalysts consist of molybdenum and cobalt (or nickel) supported on a high-surface-area porous alumina support. Cobalt oxide on alumina has shown good reactivity for the hydrodesulfurization (HDS) reaction (*8*), even though the HDS activity of $CoO–MoO_3/Al_2O_3$ is much higher (*9, 10*). Nevertheless, the CoO/Al_2O_3 catalyst system and the sulfiding reaction mechanism that occurs on its surface are not yet fully understood.

A temperature-programmed reduction (TPR) study (*11*) has shown that the structure of oxidic CoO/Al_2O_3 catalysts is unexpectedly complicated; at least four oxidic Co phases could be distinguished. Sulfiding of CoO/Al_2O_3 has been studied (*8*) by means of temperature-programmed sulfiding (TPS). Sulfiding in H_2S/H_2 (measured by TPS) is much faster than reduction in H_2 (measured by TPR). H_2S is the primary reactant in O–S exchange reactions, whereas H_2 plays only a secondary role, e.g., in reduction of elemental sulfur.

Earlier work (*12*) shows that planar model catalysts are essentially the same as their commercial porous hydrotreating counterparts. In this study, our objective was to investigate the sulfiding mechanism of CoO deposited on planar alumina. Since Co plays a major role in the catalytic activity of sulfided $Co–Mo/Al_2O_3$ catalysts (*7*), knowledge of the sulfiding mechanism of CoO on Al_2O_3 will provide some insight into the formation of active cobalt species. We present temperature-programmed desorption (TPD) and Auger electron spectroscopy (AES) results from H_2O and H_2S adsorbed on a thin film CoO/Al_2O_3 model.

2. EXPERIMENTAL

The experiments were carried out in a turbo- and cryopumped stainless-steel UHV (ultrahigh vacuum) system which has been described elsewhere (*13*). The base pressure was in the 10^{-10} Torr range. This system includes a single-pass cylindrical mirror analyzer with an electron gun for AES and a line-of-sight mass spectrometer interfaced to a computer for TPD. The temperature ramp for TPD was 3 K/s. In addition, the system includes a sputtering gun, a thermal evaporation source for cobalt, leak valves, and an ionization pressure gauge.

The Al(110) crystal (~1-cm-diameter, 2-

0021-9517/90 $3.00

mm-thick disk) was held by two 0.5-mm Ta wires which ran through grooves in the top and bottom for resistive heating. The sample was cooled to 140 K by a copper block strapped on a stainless-steel tube filled with liquid N_2. Temperature was measured using a chromel–alumel thermocouple. The thermocouple wires were spotwelded to a platinum foil and wedged into a 0.5-mm groove in the aluminum disk.

After initial cleaning, the crystal was typically cleaned by sputtering for ~10 min (*14*). The argon back-pressure was 5×10^{-4} Torr, the crystal temperature 700 K, the emission current 7 mA, the beam voltage 2 kV, and the ion beam current ~4 μA. Beam energy (3 kV) and 1-μA beam current were used for AES analysis. The procedure was repeated until no impurity was detected. The major impurity was carbon; some oxygen was added to oxidize it, followed by hydrogen to reduce the surface oxygen.

The clean Al surface was oxidized (*15–17*) at 723 K under O_2/H_2O pressure of 5×10^{-8} Torr to give an Al_2O_3 layer. Using AES (*18*), no elemental Al was detected at 68 eV. The oxidation was continued until the oxygen AES signal saturated. Under these conditions, the AES peak ratios correspond to handbook values (*19*) (Fig. 1a) for Al_2O_3. The typical oxide thickness obtained under these conditions is 50–100 Å.

The cobalt was dosed, with the substrate at room temperature, from a thermal evaporation source consisting of a 0.003-in.-diameter high-purity cobalt (99.99%) wire wrapped around a tungsten filament. The cobalt deposition was followed by AES (Fig. 1b), whose signal is commonly used to determine the coverages and growth mechanism (*13, 20–23*). The film thickness was calibrated by plotting (Fig. 2) the increase in the AES Co(775)/O(503) signal ratio as a function of cobalt deposition time. It shows discernible breaks, consistent with an approximately layer-by-layer deposition. The first break in the slope indicates the completion of the first Co monolayer. It occurs at about 1800 s and corresponds to a Co/O peak-to-peak ratio of ~0.7. The deposition of the second monolayer takes about the same time as that of the first one, indicating that the thin film grows uniformly. Clarke *et al.* (*24*) found that cobalt films also grow in a layer-by-layer mode on a Cu(001) substrate. On the other hand, Cu grows in clusters on the Al_2O_3 surface (*23*).

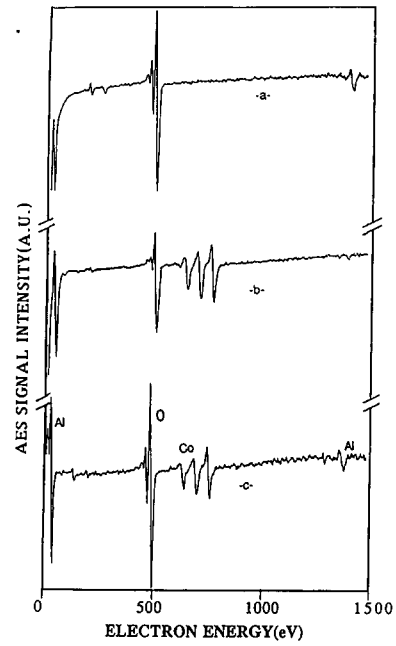

FIG. 1. Auger (3 kV) spectra of (a) Al_2O_3: A clean Al(110) sample was oxidized at 723 K under O_2/H_2O pressure of 5×10^{-8} Torr. (b) Co/Al_2O_3 prepared by thermally evaporating cobalt on Al_2O_3 (for 1800 s to obtain a monolayer), at room temperature from a 0.003-in.-diameter cobalt wire, (c) CoO/Al_2O_3 obtained by oxidizing the Co/Al_2O_3 at 700 K with an oxygen back-pressure of 5×10^{-8} Torr.

The last step in the sample preparation was the oxidation of cobalt. The sample was held at 700 K with an oxygen back-pressure of 5×10^{-8} Torr until the oxygen AES signal saturated (Fig. 1c). Under these conditions, the cobalt oxide layer is predominantly CoO (*25, 26*). However, there appears to be some clustering of CoO after oxidation, as indicated by a decrease in the Co/Al ratio.

A clean cobalt surface was prepared after each complete set of H_2O and then H_2S ex-

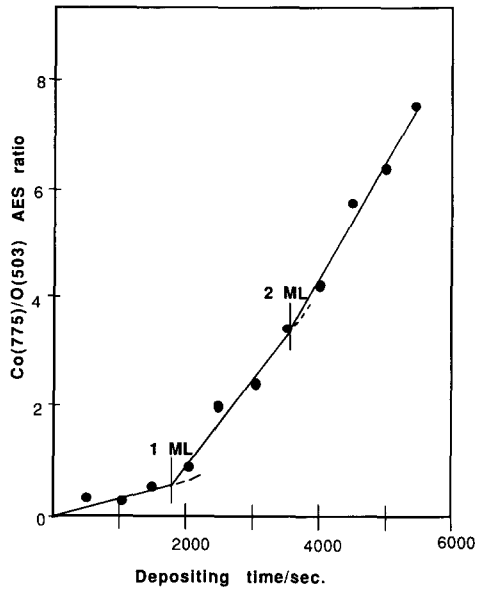

FIG. 2. Co(775)/O(503) 3-kV Auger peak-to-peak signal ratio versus cobalt vapor-deposition time. Cobalt was thermally evaporated on the alumina surface at room temperature. The evaporation source consisted of a 0.003-in.-diameter cobalt wire wrapped around a tungsten filament.

periments. Fresh Co was not added between each successive H_2S dose. While this makes effects like hydroxylation and restructuring unavoidable, the same difficulties are encountered when a single large dose is used.

3. RESULTS

Adsorption of H_2O. H_2O was adsorbed on CoO/Al_2O_3 and examined by TPD. H_2O vapor was dosed with the substrate at 140 K. The thickness of the cobalt oxide film of this sample corresponds to about one monolayer. Prior to the dosing of H_2O, the sample was flashed up to 700 K. Blank TPD did not exhibit any water desorption. This was predictable, since the system was cryopumped and therefore the water background was negligible. For different doses of H_2O, five main peaks can be observed (Fig. 3), each of them corresponding to a different type of water–oxide interaction.

For doses of 3 Langmuirs (L) or below (not shown), the absence of TPD peaks suggests water dissociation on the oxidized cobalt film-forming hydroxyl groups. This structure is probably stable at $T < 600$ K. For higher doses, the peak at 450 K is most likely due to the recombination of the hydroxyl groups from the water decomposition. This TPD peak temperature and its interpretation are consistent with the data of Takita *et al.* (*27*), who concluded that, for H_2O on Co_3O_4, the hydroxyl recombination peak appeared at 500 K. Earlier work (*28, 29*) indicates that water dissociates to form hydroxyls on the atomically rough surfaces of clean cobalt. Others (*30–32*) have concluded that H_2O dissociation occurs very easily on aluminum oxide surfaces. One report (*32*) found that dissociation occurs even at 150 K on Al_2O_3.

For doses less than 32 L, no detectable water desorption was observed between 140 and 160 K, whereas for higher doses (>30 L), TPD shows a peak between 150 and 160

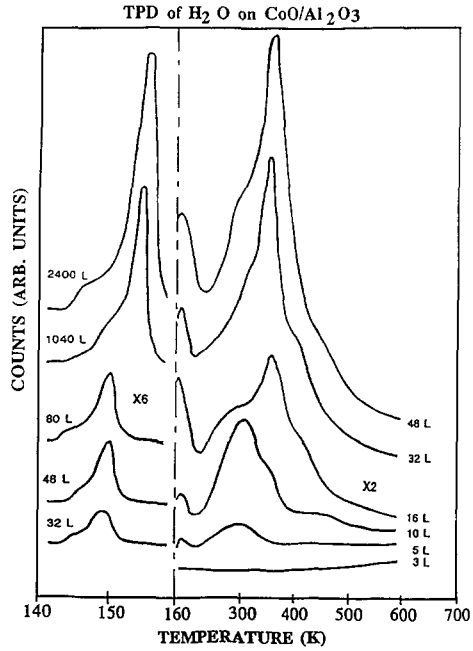

FIG. 3. TPD spectra of H_2O after H_2O exposures (as labeled) on CoO/Al_2O_3. The water was dosed at 140 K on 1 monolayer CoO on Al_2O_3 surface. The temperature ramp rate was 3 K/s. For all spectra, the *y*-axis scale is three times larger between 140 and 160 K than that between 160 and 700 K.

K, with a shoulder at 145 K. Desorption from this state exhibits zero-order kinetics and a lack of saturation. These two observations support the assignment of this state as due to ice multilayers where sublimation is a zero-order process. Thermal desorption states of ice multilayers are identified under similar conditions on many other metal and oxide surfaces. Heras *et al.* (*33*) observed a comparable peak for water on cobalt but concluded from LEED results that H_2O is adsorbed without long-range order at low temperature. On alumina powders (*34*) water can adsorb in multilayer states under favorable conditions of temperature and pressure. The shoulder at 145 K is discussed below.

For doses of 5 L and higher, a peak at 170 K is resolved and can be assigned to molecular water which is stabilized by its direct attachment to the surface. Such states are also reported for H_2O on other oxidized surfaces, for instance, on ZnO (*35*), on anatase (*36*), and also on metal surfaces including Pt(111) (*37*) and Ru(001) (*38*). Beginning at 5 L, and growing in with the 170 K peak, are several peaks above 250 K. The first two peaks (between 300 and 400 K) correspond to molecular water adsorbed on different sites. The high desorption temperature is surprising. It is attributed to the oxide substrate–H_2O interaction in which H_2O bonds to specific cation sites. It has been suggested that this occurs, for instance, on ZnO (*35*), Ti_2O_3 (*39*), and TiO_2 (*36*). On clean metal surfaces, the molecularly chemisorbed water desorption occurs below room temperature (*40*), usually between 200 and 250 K. On cobalt, chemisorbed water desorbs with a 155 K TPD peak (*33*).

Adsorption of H_2S. Using a procedure similar to that used for water, the reaction of H_2S with CoO/Al_2O_3 has been studied. H_2S vapor, with no detectable impurity, was dosed repeatedly onto a cobalt oxide film (~1 monolayer thick) at 140 K. No cleaning was performed between doses.

Figure 4 shows two representative AES spectra taken after TPD measurements (corresponding to two different H_2S doses: 100 and 6000 L). The presence of a S AES peak is strong evidence for the decomposition of H_2S on the surface and should be compared to the clean surface in Fig. 1c. This is in good agreement with earlier H_2S/CoO work (*41*), which indicates a gain of sulfur and a loss of oxygen on CoO surfaces. This is presumably because sulfur is a more covalent ligand than oxygen (*7*); the thermodynamics also favor H_2O formation. Slager and Amberg (*42*) arrived at the same conclusions using alumina. For the 100-L H_2S dose spectrum, the S(152)/Co(775) AES peak-to-peak ratio is 1.64. By including the relative Auger sensitivity factors (*19*) the surface S/Co atomic ratio is 0.52. The AES peak-to-peak signal ratio of Co(775)/O(503) is 0.23 and remains constant throughout the whole dosing experiment. This can be understood because virtually all of the AES oxygen signal originates from the alumina underneath the cobalt oxide layer. Therefore, within our detection limits, the loss of oxygen in the cobalt oxide layer does not affect this ratio. For the 6000-L H_2S dose spectrum, the S(152)/Co(775) AES peak-to-

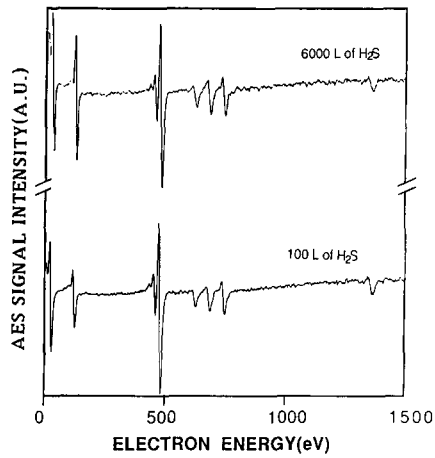

FIG. 4. AES 3-kV spectra of 1 monolayer of CoO on Al_2O_3 after two different cumulative H_2S doses at 140 K (i.e., 100 and 6000 L) with no cleaning between doses. The AES spectra were taken at room temperature after TPD.

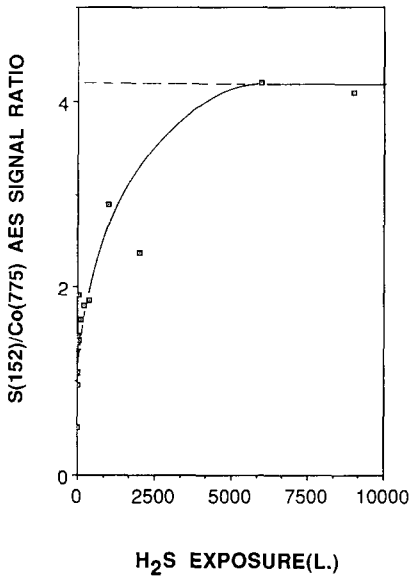

FIG. 5. Auger (3 kV) S(152)/Co(775) peak-to-peak height ratio as a function of H_2S exposure (at 140 K) to CoO/Al_2O_3 with no cleaning between doses. The AES spectra were taken at room temperature after TPD.

peak ratio is 4.2 and represents a S/Co atomic ratio of 1.33.

In Fig. 5 all the calculated S(152)/Co(775) AES peak-to-peak signal ratios corresponding to different H_2S doses are plotted versus H_2S exposure. One can observe a very fast rise (for exposure <800 L) and a slower rise for higher doses. For a cumulative H_2S dose of 6000 L, the S/Co AES signal ratio saturates at ~4.

The only TPD products detected were water and H_2S; no significant amounts of H_2 were desorbed. Following H_2S adsorption at 140 K, thermal desorption of the formed water was a strong function of H_2S exposure. In Fig. 6, the TPD of water exhibits four peaks at 145, 150, 300, and 400–450 K. The 145 and 150 K peaks correspond to physisorbed states in which the water product is weakly bonded either to the surface or to other water-derived species. The shift to lower temperature for higher doses of H_2S corresponds to the progressive replacement of the oxidic oxygen on the surface by elemental sulfur from decomposed H_2S. The 300 K peak corresponds to chemisorbed molecular water that has formed. This peak shifts to lower temperatures for higher H_2S doses. The 400–450 K peak is attributed to the recombination of OH groups. When the sample is sulfur free (low H_2S dose), this temperature corresponds approximately to that observed in water dosing. It shifts to lower temperature when the dose is increased.

Once the surface was saturated with sulfur, we sputtered the sample until no more sulfur was detectable by AES (Fig. 7a), then heated it to 700 K for a few minutes; sulfur was observed again by AES (Fig. 7b). Similar heating of the clean sample did not show any sulfur. Additionally, no trace of sulfur was detected after argon sputtering (Fig. 7a). The knock-on effect can thereby be neglected. Therefore, observed sulfur in Fig. 7b is believed to be diffused sulfur from the

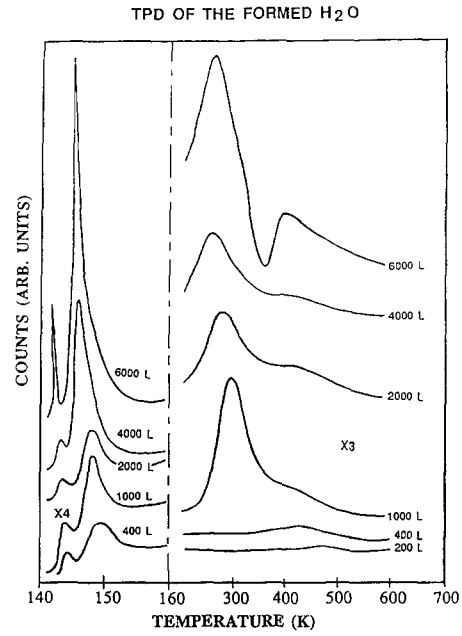

FIG. 6. TPD spectra of formed water resulting from different H_2S exposures (as labeled) at 140 K on 1 monolayer of CoO on Al_2O_3. The temperature ramp rate was 3 K/s. The x-axis scale is ~12 times larger between 140 and 160 K than that between 160 and 700 K. No water was observed on blank TPD.

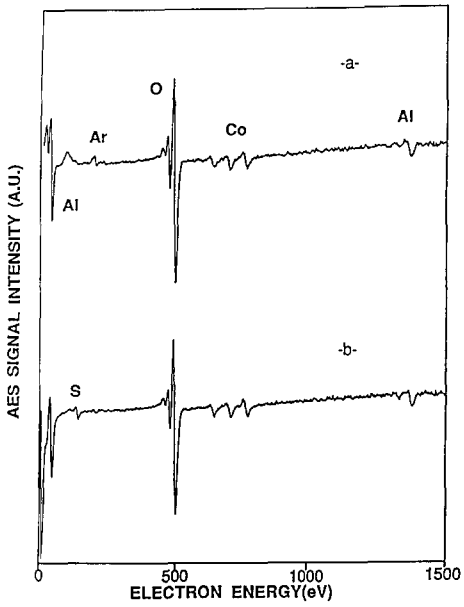

FIG. 7. Auger (3 kV) spectra of two cleaning process steps of sulfur-saturated sample (a) after sputtering until no more sulfur was detectable with an ~4-μm ion beam current and (b) after heating this sputtered sample up to 700 K for ~10 min.

bulk alumina. The possibility of subsurface sulfur adsorption (in addition to the adsorbed surface monolayer) has been proposed by Weeks and Plummer (*43*) on a Ni(100) surface.

The TPD of H_2S (Fig. 8), obtained by dosing H_2S at 140 K, exhibits two resolvable states (TPD peaks at 200 and 240 K) which could be attributed to weakly held molecular H_2S in contact with already adsorbed H_2S, as observed for instance by Zhou and White (*44*) on Ni(100), and a monolayer molecular adsorption state, respectively. Earlier work on H_2S on rutile (*36*) exhibits the same TPD peaks. The temperature of the monolayer peak can be compared to that of H_2S on other surfaces: on Rh(100) (*45*) between 220 and 300 K, and on rutile and anatase (*36*) at 250 and 300 K, respectively.

4. DISCUSSION

Considering all the results together, the picture that emerges is the replacement of the surface oxygen ion by sulfur from H_2S which results in the formation of water. The cobalt oxide is thereby progressively sulfided.

Slager and Amberg (*42*) indicate that H_2S decomposition on alumina proceeds in two steps: decomposition of H_2S with formation of OH groups and recombination to form water. Hair (*34*) indicates that hydroxyl groups are stable up to ~1000 K on aluminum oxide surfaces. If we assume that H_2S decomposes more readily on exposed alumina than on CoO, the absence of water desorption for H_2S doses below 200 L (Fig. 6) can be understood. Above 200 L, when the alumina sites are saturated with H_2S decomposition products, H_2S starts to react on CoO sites to form OH, which recombines at 450 K (Fig. 3). The low-temperature TPD peaks for >400-L H_2S doses (Fig. 6) suggest that on CoO the water formation does not

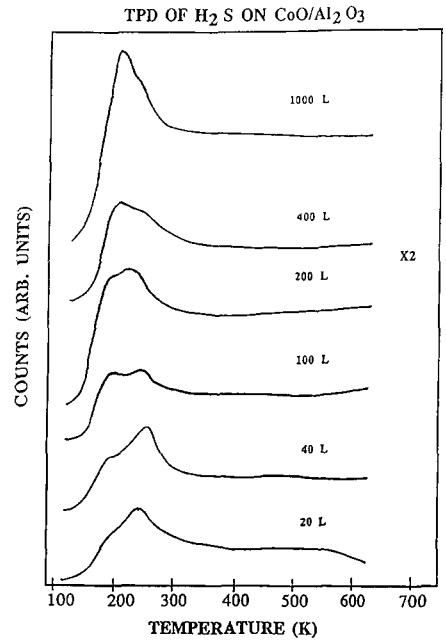

FIG. 8. TPD spectra of H_2S for various H_2S doses (as labeled) at 140 K on 1 monolayer CoO on Al_2O_3. The temperature ramp rate was 3 K/s. The rising background is attributed to the slow pumping speed of H_2S and to desorption from the sample mounting assembly.

proceed via the recombination of OH groups, as it does on alumina. It seems instead to involve a direct reaction of H_2S with lattice oxygen ions to form free water molecules and sulfur, similar to the behavior on MgO (*46*). These arguments are in good agreement with Fig. 5, where we observed two different sulfur deposition rates. The fast one (for doses <400 L) probably corresponds to the H_2S decomposition and the much slower one (for higher doses) to the H_2S decomposition and formation of water. Therefore the oxide surface sulfurization proceeds in two steps consisting of adsorption and decomposition of H_2S on the surface with formation of hydroxyl groups and then, above a critical sulfur coverage, reduction of the oxide with formation of water.

Additionally, in Fig. 6 the two peaks at 145 and 150 K indicate a highly reactive surface: The formation of water must occur below these temperatures. Koestner *et al.* (*47*) indicate that H_2O does not decompose on Pt(111) below 180 K, although H_2S readily forms atomic sulfur on the same surface at 110 K. According to Fig. 8, no H_2S desorption is observed below 160 K. Therefore, the adsorbed H_2S is believed to react with the oxygen from CoO to form water, probably at the dosing temperature (i.e., 140 K). The water can then be adsorbed at different sites on the partially sulfided cobalt oxide surface. Mitchell *et al.* (*48*) found that the desorbing water resulting from the reaction of H_2S on oxygen-covered platinum (111) is fully formed below 170 K.

The 150 K (and 145 K) water desorption peaks in Figs. 3 and 6 suggest that the formed molecular water interacts by hydrogen bonding with either the anion (O^{2-}) of the oxide, the hydroxyl groups, or the already formed molecular water (Fig. 9, type 2). The 145 K desorption peak (Fig. 6) appears with much lower intensity under the experimental conditions of Fig. 3; therefore, some weak interactions that did not exist with the nonsulfided surface must be present. Possibly, hydrogen bonding of the chemisorbed formed water with surface sulfide is the cause (Fig. 9, type 1).

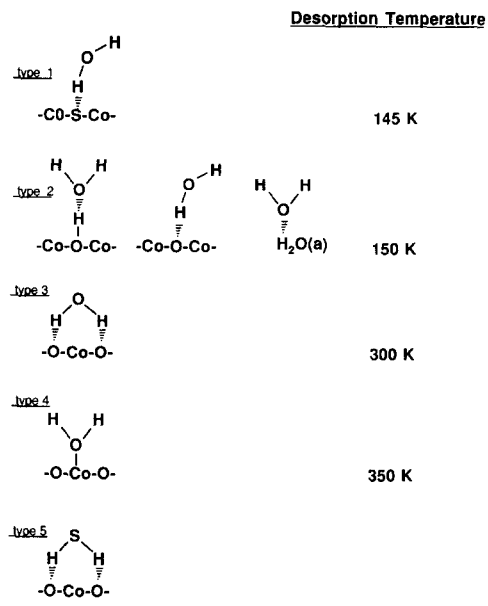

FIG. 9. List of different water adsorption sites with their approximate desorption temperatures.

Adsorbed H_2S desorbs with peaks at 200 and 250 K (Fig. 8). At 300 K and above, the H_2S desorption is complete and the surface can be considered H_2S-free. However, water desorption occurs above 300 K under these conditions (Fig. 6). This indicates that water, corresponding to the 300 and 350 K desorption peaks, was formed below 250 K. It is possible that the water desorbing from these peaks was also formed at 140 K. In Fig. 3, at low coverage (<10 L), the 300 K peak is larger than that at 350 K. Starting at 16 L and for higher doses, the 350 K peak becomes more and more important compared to that at 300 K. From these considerations, we could attribute the 350 K peak to chemisorbed water bound to a cobalt atom (Lewis acid) (Fig. 9, type 4) and the 300 K peak to the water interacting with two surface oxygen anions by hydrogen bonding (Fig. 9, type 3). Water adsorption on these sites is favored at low H_2O doses in compari-

son to the chemisorbed sites on top of Co atoms. But the type 3 sites, composed of two adjacent surface oxygen atoms, saturate more quickly than the cobalt atom sites for monolayer interactions. The TPD of formed water (Fig. 6) does not exhibit the two peaks around 300 K that we see in Fig. 3 for the dosed water. This can be explained if, for each H_2S molecular decomposition, one surface oxygen anion is replaced by a sulfide and, thereby, four potential type 3 sites are obstructed. Sulfur adsorbs very readily on the surface even at low doses; therefore, the absence of a peak corresponding to this interaction is understandable in Fig. 6. Deane *et al.* (*46*) indicate, in a study of H_2O on MgO, that very little H-bonded water appears in the IR spectra of the surface after reaction of H_2S. We notice, in Fig. 8, the absence of a peak corresponding to the H_2S state interacting with two hydrogen bonds to the surface oxygen anions (Fig. 9, type 5). No evidence was found in the literature for such H_2S interaction on oxided surfaces. A study of H_2S on magnesium oxide by infrared spectroscopy (*46*) indicates the presence of double H-bonded water (Fig. 9, type 3) but no H_2S interaction (type 5). The difference in chemisorbed water peak temperatures between Fig. 3 (350 K) and Fig. 6 (300 K) is attributed to the progressive sulfidation of the surface, which weakens the Co–H_2O interaction.

In Fig. 3, between 16 and 48 L, the monolayer peak continues to grow even after the multilayer sets in. This can be explained by the formation of multilayer islands or clusters which leave exposed oxide for further monolayer growth while simultaneously showing growth of the multilayer. On oxides, H_2O generally forms hydrogen-bonded clusters at high coverage, for example with Ti_2O_3 (*39*), because the oxide substrate–H_2O interaction, which ties H_2O to specific cation sites, can override the strong tendency to cluster that we see on clean metal surfaces (*40*).

The surface reaction may proceed according to one (or both) of the following steps:

$$H_2S(g) + O^{2-}(s) = H_2O(g) + S^{2-}(s) \quad (1)$$

$$H_2S(g) + 2O^{2-}(s) = 2OH^- + S^{2-}(s). \quad (2)$$

Equation (1) represents the direct exchange of a sulfur atom with a lattice oxygen ion to form a free water molecule; the water can then react in the normal way. This reaction is believed to occur predominantly on cobalt sites at the dosing temperature (i.e., 140 K). The exchange of lattice oxygen ion with sulfide from adsorbed H_2S, resulting in water formation, has been proposed for many other systems, notably H_2S on MgO (*46*), on TiO_2 (*36*), and on alumina (*42, 49*). Kinetic studies (*50*), reveal that rates of H_2S decomposition on metals are generally very rapid, the high sticking probability suggesting that there is no barrier to adsorption and dissociation. An alternative form [Eq. (2)] produces hydroxyl groups that recombine to form water between 400 and 450 K. This reaction is believed to predominate on alumina-exposed sites at low H_2S (<400 L) doses before water formation.

A comparison of the free energies of formation of CoO, CoS, H_2O, and H_2S (*51*) shows that while CoO is ~25 kcal/mol more stable than CoS, H_2O is ~50 kcal/mol more stable than H_2S. The thermodynamic driving force of the reaction is the formation of water from H_2S.

5. SUMMARY

H_2S adsorbs and decomposes readily on the CoO/Al_2O_3 surface at 140 K. After a critical exposure, this decomposition leads to a progressive replacement of oxygen ions on the surface by sulfide, strongly bonded to the surface. Water is also formed, presumably at 140 K. The formed water TPD has some strong similarities to directly dosed water TPD. Nevertheless, some new peaks can be observed in the former. Globally, on the partially sulfided cobalt oxide surface, water can occupy (a minimum of) six different sites (*52*), as listed in Fig. 9 with

their respective desorption temperatures. The remaining sulfur can diffuse into the bulk alumina underneath.

ACKNOWLEDGMENT

This work was supported by the U.S. Department of Energy, Office of Basic Energy Sciences, and by the Robert A. Welch Foundation. T. Sahin acknowledges the support of U.S. Department of Energy Pittsburgh Energy Technology Center. We also acknowledge many fruitful discussions with Dr. M. Steinberg, Dr. F. Solymosi, Dr. E. L. Hardegree, and Dr. S. Akhter. One of us (E.A.) thanks the Robert A. Welch Foundation for a Fellowship.

REFERENCES

1. Arnoldy, P., De Booys, J. L., Scheffer, B., and Moulijn, J. A., *J. Catal.* **96,** 122 (1985).
2. Cocke, D. L., *Catal. Rev.-Sci. Eng.* **26,** 163 (1981).
3. Hayden, T. F., and Dumesic, J. A., *J. Catal.* **103,** 366 (1987).
4. Massoth, F. E., *J. Catal.* **36,** 164 (1975).
5. Schrader, G. L., and Cheng, C. P., *J. Catal.* **85,** 488 (1984).
6. Scheffer, B., De Jonge, J. C. M., Arnoldy, P., and Moulijn, J. A., *Bull. Soc. Chim. Belg.* **93,** 751 (1984).
7. Topsøe, H., and Clausen, B. S., *Appl. Catal.* **25,** 273 (1986).
8. Arnoldy, P., Van Den Heukant, J. A. M., De Bok, G. D., and Moulijn, J. A., *J. Catal.* **92,** 35 (1985).
9. Wivel, C., Candia, R., Clausen, B. S., Mørup, S., and Topsøe, H., *J. Catal.* **68,** 453 (1981).
10. De Beer, V. H. J., Van Sint Fiet, T. H. M., Van Der Steen, G. H. A. M., Zwaga, A. C., and Schuit, G. C. A., *J. Catal.* **35,** 297 (1974).
11. Arnoldy, P., and Mouljin, J. A., *J. Catal.* **93,** 38 (1985).
12. Sahin, T., Gokce, H., and Ford, W. K., *in* "Catalysis 1987," (J. W. Ward, Ed.), pp. 503–512. Elsevier, Amsterdam, 1988.
13. Zhou, X. L., Yoon, C., and White, J. M., *Surf. Sci.* **203,** 53 (1988).
14. Musket, R. G., Colmenares, W., Makowiecki, D. M., and Siekhaus, W. J., *Appl. Surf. Sci.* **10,** 143 (1982).
15. Belton, D. N., and Schmieg, S. J., *Appl. Surf. Sci.* **32,** 173 (1988).
16. Michel, R., Jourdan, C., Castaldi, J., and Derrien, J., *Surf. Sci.* **84,** L509 (1979).
17. Chen, J. G., Crowell, J. E., and Yates, J. T., *Surf. Sci.* **185,** 373 (1987).
18. Madden, H. H., and Goodman, D. W., *Surf. Sci.* **150,** 39 (1985).
19. Palmberg, P. W., Riach, G. E., Weber, R. E., and MacDonald, N. C., "Handbook of Auger Electron Spectroscopy." Physical Electronics Industries, Inc., 1972.
20. Biberian, J. P., and Somorjai, G. A., *Appl. Surf. Sci.* **2,** 352 (1979).
21. Seah, M. P., *Surf. Sci.* **32,** 703 (1972).
22. Paunov, M., and Bauer, E., *Surf. Sci.* **188,** 123 (1987).
23. Di Castro, V., and Polzonetti, G., *Surf. Sci.* **189,** 1085 (1987).
24. Clarke, A., Jennings, G., Willis, R. F., Rous, P. J., and Pendry, J. B., *Surf. Sci.* **187,** 327 (1987).
25. Gulbransen, E. A., and Hickman, J. W., *Trans. AIME* **171,** 306 (1947).
26. Arkharov, V. I., and Voroshilova, Z. A., *Zh. Tekh. Fiz.* **6,** 781 (1936).
27. Takita, Y., Tashiro, T., Saito, Y., and Hori F., *J. Catal.* **97,** 25 (1986).
28. Heras, J. M., and Albano, E. V., *Surf. Sci.* **7,** 332 (1981).
29. Moyes, R. B., and Roberts, M. W., *J. Catal.* **49,** 216 (1977).
30. Paul, J., and Hoffmann, F. M., *J. Phys. Chem.* **21,** 5321 (1986).
31. Almy, D. B., Foyt, D. C., and White, J. M., *J. Electron Spectrosc.* **11,** 129 (1977).
32. Chen, J. G., Crowell, J. E., and Yates, J. T., *J. Chem. Phys.* **84,** 5906 (1986).
33. Heras, J. M., Papp, H., and Spiess, W., *Surf. Sci.* **117,** 590 (1982).
34. Hair, M. L., "Infrared Spectroscopy in Surface Chemistry." Dekker, New York, 1967.
35. Zwicker, G., and Jacobi, K., *Surf. Sci.* **131,** 179 (1983).
36. Beck, D. D., White, J. M., and Ratcliffe, C. T., *J. Phys. Chem.* **90,** 3123 (1986).
37. "Monolayer and Multilayer Adsorption of Water on the Pt(111) Surface." General Motors Research Publication No. GMR-4007/PCP-171, 1982.
38. Doering, D., and Madey, T. E., *Surf. Sci.***123,** 305 (1982).
39. Kurtz, R. L., and Henrich, V. E., *Phys. Rev. B* **26,** 6682 (1982).
40. Thiel, P. A., and Madey, T. E., *Surf. Sci. Rep.* **7,** 211 (1987).
41. Dumas, P., Steinbrunn, A., and Colson, J. C., *C.R. Acad. Sci. Paris* **287,** 26 (1978).
42. Slager, T. L., and Amberg, C. H., *Canad. J. Chem.* **50,** 3416 (1972).
43. Weeks, S. P., and Plummer, E. W., *Chem. Phys. Lett.* **48,** 601 (1977).
44. Zhou, Y., and White, J. M., *Surf. Sci.* **183,** 363 (1987).
45. Hedge, R. I., and White, J. M., *J. Phys. Chem.* **90,** 296 (1986).
46. Deane, A. M., Griffiths, D. L., Lewis, I. A., Winter, J. A., and Tench, A. J., *J. Chem. Soc. Farad. Trans. 1* **75,** 1005 (1975).
47. Koestner, R. J., Salmeron, M., Kollin, E. B., and Gland, J. L., *Surf. Sci.* **172,** 668 (1986).
48. Mitchell, G. E., Schulz, M. A., and White, J. M., *Surf. Sci.* **197,** 379 (1988).

49. Liu, C. L., Chuang, T. T., and Dalla Lana, I. G., *J. Catal.* **26,** 474 (1972).
50. Bartholomew, C. H., Agrawal, P. K., and Katzer, J. R., *in* "Advances in Catalysis" (D. D. Eley, H. Pines, and P. B. Weisz, Eds.), Vol. 31, p. 135. Academic Pess, San Diego, 1982.
51. Karapet'yants, M. KH., and Karapet'yans, M. L. "Thermodynamic Constants of Inorganic and Organic Compounds. Ann Arbor–Humphrey Science publishers, Ann Harbor, MI, 1970.
52. H. Knözinger, *in* "The Hydrogen Bond" (P. Schuster, G. Zundel, and C. Sandorfy, Eds.), Vol. 3, pp. 1263–1364. North Holland, Amsterdam, 1976.